Available online at www.sciencedirect.com
SCIENCE DIRECT
Polymer 46 (2005) 9476–9488
polymer
www.elsevier.com/locate/polymer

Interparticle and particle–matrix interactions in polyethylene reinforcement and viscoelasticity

Maged A. Osman*, Ayman Atallah[1]

Department of Materials, Institute of Polymers, ETH Zurich, Wolfgang-Pauli-strasse 10, CH-8093 Zurich, Switzerland

Received 26 April 2005; received in revised form 30 June 2005; accepted 8 July 2005
Available online 8 August 2005

Abstract

Composites of surface treated and untreated non-colloidal $CaCO_3$ particles and high-density polyethylene (HDPE) with different filler loading (0–30 vol%) were prepared. Their viscoelastic properties were studied by dynamic strain sweep and small amplitude oscillatory shear and correlated to the particle–particle and particle–matrix interactions. The results gave insight into the mechanism of polymer reinforcement by solid inclusions and the factors that lead to the often observed solid-like response in the terminal zone. With increasing filler volume fraction, the particles tend to agglomerate and build clusters (local structures) that can be disintegrated by shearing. Up to 30 vol% no evidence for a space-filling particle network could be found. The presence of clusters increases the viscosity, the moduli and the viscoelastic non-linearity of the composites. Coating the filler surface by a stearic acid monolayer reduces its tendency to agglomerate as well as the adhesion between the particles and the polymer, leading to lower viscosity and interfacial slippage with increasing strain amplitude. Solid inclusions increase the storage modulus more than the loss modulus, hence decrease the material damping. The hydrodynamic reinforcement is frequency independent and dominates at high frequency. Polymer adsorption on the particles surface results in a transient filler–polymer network, which together with the topological restraints exerted by the inclusions on the polymer chain reptation leads to slow relaxation. These slow relaxation processes are sensitive to the oscillation frequency and strongly contribute to the polymer reinforcement at low frequencies. Agglomerates differ in shape and packing from the nearly spherical primary particles, and exert strong restraints on the polymer chain relaxation, hence offer an additional contribution to the composite's moduli. The sum of these effects results in higher moduli and a shift of the crossover (liquid-like to solid-like) frequency to lower values with increasing filler volume fraction. They also lead to the often-observed tendency towards a solid-like response in the terminal zone before a space-filling filler network is formed. Hydrodynamic and micromechanical models can only predict the hydrodynamic reinforcement, provided that the polymer strongly adheres to the inclusions.

Keywords: Polyethylene; Reinforcement; Calcite

1. Introduction

Polyolefins are widely exploited but are often not used as neat polymers. To enhance their properties, they are frequently compounded with natural minerals. A prominent goal of filler addition is mechanical reinforcement. Calcite is the most abundant mineral on earth and polyethylene (PE)-calcite composites are, therefore, of considerable industrial interest. Filler particles often build agglomerates (soft flocks) or aggregates (hard agglomerates that require attrition to be disintegrated) with increasing volume fraction, depending on their surface area and energy. These soft or hard clusters strongly influence the mechanical properties (stiffness, strength, ductility) and the viscoelasticity of the composites. In the first part of this investigation, it was shown that the steady state shear viscosity is quite sensitive to the presence of agglomerates and offers a reliable indicator for filler dispersion [1].

In the solid-state, the properties of composite materials are determined by those of the components, the shape and volume fraction of the filler as well as by the morphology of the system and the nature of the interphase. In the melt, changes in morphology originating from polymer crystallization can be excluded and the influence of the other factors on the composite properties can be studied. Rheological

* Corresponding author. Tel.: +41 44 6324653; fax: +41 44 6321096.
E-mail address: mosman@mat.ethz.ch (M.A. Osman).
[1] Present address: Physics Department, Faculty of Science, Cairo University-Bani Suef Branch, Egypt.

0032-3861/$ - see front matter © 2005 Elsevier Ltd. All rights reserved.
doi:10.1016/j.polymer.2005.07.030

measurements, especially oscillatory shear, can give insight into the influence of filler dispersion, volume fraction and particle–matrix interaction on the dynamic mechanical properties. A useful tool to explore the behavior of complex fluids under stress without significantly deforming its microstructure is small-amplitude oscillatory shear.

The fundamental analogy between the hydrodynamics of suspensions and the elastostatics of incompressible solids with solid inclusions has been pointed out [2]. Many of the equations, which predict the moduli of composites, have their origin in the theory of suspension viscosity (hydrodynamic models) and analogous equations hold for shear modulus, G, and viscosity, η [3–5]. That is, as long as the deformation is small, $\eta/\eta_1 = G/G_1$, where the subscript 1 denotes the polymer matrix. Equations developed to calculate the change in reduced viscosity with increasing filler volume fraction usually hold for the reduced modulus, e.g. Guth–Smallwood Eq. (1) for spherical particles (intrinsic viscosity $[\eta]=2.5$),

$$G = G_1(1 + 2.5\phi_2 + 14.1\phi_2^2) \tag{1}$$

where ϕ is the volume fraction and the subscript 2 denotes the dispersed phase. However, this is only adequate, when Poisson's ratio of the continuous phase (ν_1) is 0.5 and the rigidity of the filler is much greater than that of the matrix, which is the case in calcite filled polymer melts. An empirical expression, which is often successfully used to describe the viscosity of non-interacting suspensions but less frequently used to estimate the modulus, is the Krieger–Dougherty Eq. (2) [6–8]

$$\eta_r = \frac{\eta}{\eta_1} = \left(1 - \frac{\phi_2}{\phi_{max}}\right)^{-[\eta]\phi_{max}} \tag{2}$$

where ϕ_{max} is the particle maximum packing fraction (true volume/apparent volume) and $[\eta]$ is the intrinsic viscosity (a measure of the effect of individual particles on the viscosity, reflecting the influence of particle shape, orientation and interaction with the fluid). This function, which reduces to the Einstein equation in dilute suspensions (<2 vol%), allows $[\eta]$ and ϕ_{max} to vary with the shear stress, hence accounting for shear thinning. If this equation is used to estimate the shear modulus, the intrinsic shear modulus $[G]$ replaces $[\eta]$ [9,10].

Micromechanical relationships have been developed to predict the moduli of polymers filled with spherical particles and were extended to anisometric inclusions [11–16]. The Kerner [11] equation and its modifications, e.g. Hashin–Shtrikman [12] or Halpin–Tsai [13] are often used to estimate the shear modulus of composites. A simplified form of the Kerner equation is:

$$\frac{G}{G_1} = \frac{1}{G_1}\left[1 + \frac{15(1-\nu_1)\phi_2}{(7-5\nu_1)\phi_1}\right] \tag{3}$$

Nielsen [14–16] introduced the concept of maximum packing and generalized the Kerner equation further to:

$$\frac{M}{M_1} = \frac{(1 + AB\phi_2)}{(1 - B\psi\phi_2)} \tag{4}$$

where M is any modulus, A is a parameter that takes the geometry of the particles and Poisson's ratio of the matrix into account. For spherical particles in a matrix with $\nu_1 = 0.5$, $A = k - 1 = 1.5$ (k is the Einstein coefficient) but becomes larger if the particles are not well dispersed (agglomerated or aggregated). The constant B takes the elastic constants of the filler and the matrix into account (its value is one for large filler/matrix ratios) and the factor ψ depends on ϕ_{max} of the filler. An empirical function, which fulfills the necessary boundary conditions, is:

$$\psi = 1 + \frac{1 - \phi_{max}}{\phi_{max}^2}\phi_2 \tag{5}$$

Accordingly, the modulus of a composite depends on the moduli of the components and their Poisson's ratio as well as on the volume fraction of the dispersed phase but is independent of the size of the inclusions. Discrepancies between theory and experiment have been frequently reported and the modulus reinforcement is often far larger than can be explained by simple micromechanical models [15,17–19]. The Kerner and similar equations assume perfect dispersion of the particles and good adhesion between the filler and the polymer matrix, that is, no relative movement of the two phases across their interface under the applied force. However, at high stresses the frictional forces between the two phases may be exceeded and the adhesion force is overcome, especially when the particle–matrix interactions are weak. Furthermore, all models assume well dispersed (no agglomeration) spherical inclusions, which is not always the case.

The mechanism of polymer reinforcement by fillers is not yet fully understood and is the subject of many publications; several important contributions stem from research on filled elastomers [20–29]. This is due to the complex microscopic interactions that control the macroscopic material response and to rearrangements in the microstructure during deformation. Elastomers and polymer melts display similar filler effects on the dynamic mechanical properties, although the elastomers recovery may be different due to their chemical cross-links. Micro- and nano-sized particles greatly increase the dynamic moduli of polymer melts and reduce the strain amplitude, corresponding to the onset of non-linear behavior as they do in elastomers [14,30]. Essentially, four factors influence the flow characteristics of a complex fluid and contribute to the shear modulus of a polymer composite: Matrix properties, hydrodynamic effects, and particle–matrix and particle–particle interactions [24]. Fluid dynamic effects, caused by the presence of solid particles in the melt stream dominate the forces exerted on the particles and the global straining motion is concentrated in the interstitial fluid. The interparticle interactions originate from electrostatic and Van der Waal's forces that can lead to agglomerates or

aggregates (sometimes with fractal structures). Below the percolation limit, these are clusters and in this context we refrain from using the word 'network' unless a space-filling structure is present. With increasing strain amplitude, de-agglomeration and breakdown of such structures may occur, leading to reduction in the dynamic storage modulus that is called 'Payne effect' in filled elastomers [20]. The polymer–particle interactions refer to the attachment–detachment process of chains adsorbed to the filler surface that is controlled by adhesion forces. The adsorbed polymer chains, whose dynamics are presumably different from the bulk-polymer, result in additional junctions beside the entanglements of polymer chains [31,32]. These additional junctions that are of different strength and lifetime from chain entanglements lead to a filler–polymer network often referred to as 'dynamic' or 'transient'. Stress-induced de-bonding of polymer chains from the filler surface breaks this filler–polymer network and contributes to the viscoelastic non-linearity with strain [25,33,34]. Hence, the interfacial interactions between the polymer and the filler contribute to the stress increment by influencing the flow deformation of the polymer melt. The bonding and de-bonding of polymer chains on filler surfaces and the effect on viscoelasticity has been studied and modeled [29,33,35]. At high filler loading and small interparticle distances (nanoparticles), direct bridging between the particles or aggregates through adsorption of polymer chains may also occur [29,36]. Whether the main contribution to the viscoelastic non-linearity comes from the break down of filler clusters or filler–polymer network has been debated [25,29].

Particulates evidently increase the dynamic moduli and viscosity of polymer melts over the whole range of frequencies and shear rates. A significant increase of the linear viscoelastic moduli and a decrease of their frequency dependence are often observed in the low frequency region for dispersions of sub-micron particles at low filler concentrations [37–41]. Similar behavior was observed in a suspension of micron-sized glass particles in poly (dimethyl siloxane), however, at a much higher concentration [30]. The observed low-frequency plateau (solid-like response) has been often attributed to the presence of a particle network [38,40,41]. In a different point of view, the solid-like response is attributed to polymer adsorption on the filler surface that provides localized junctions, and the resulting entrapped entanglements [25]. The filler volume fraction at which this plateau is observed depends on the particle size, the interfacial tension and the stiffness of the particles [27,42]. As the filler surface energy and the adhesion force between the two phases become weak due to surface treatment of the filler or to the use of polymer beads, the viscosity and dynamic moduli decrease [42–44]. Lower particle surface energy reduces the particles' tendency to agglomerate as well as the attraction forces between them and the polymer, leading to lower viscosity. Stress-induced interfacial slip may occur in such cases, that is, the filler surface becomes slippery and the enhancement of polymer flow deformation by the undeformable filler is minimized [45,46]. Interfacial slip occurs instantaneously once a critical stress is exceeded but the stick hydrodynamic boundary condition is restored once the stress is withdrawn. This underlines the necessity of using fillers with clean surfaces in rheological studies. However, the surface of commercially available calcite fillers is often contaminated with the surfactants used as milling additives [47].

In the present study, a micron-sized calcite powder with a clean surface (free of milling additives) was prepared, coated with a monolayer of stearic acid and compounded (treated and untreated) with linear high-density polyethylene (HDPE) at different filler loading. The role of interparticle and particle–matrix interactions in determining the dynamic moduli and viscosity of filled-polymers was studied by a series of oscillatory shear experiments, in order to get insight into the reinforcement mechanism of filled polymers.

2. Experimental

HDPE-calcite ($D_{v0.5}=1.85$ μm) composites containing different filler volume fractions (0–30 vol% at RT) with and without filler surface treatment were prepared. Above 30%, it was difficult to homogeneously distribute the untreated calcite in the polymer matrix. ϕ_2 was calculated using the densities of calcite and HDPE, which gives the volume of the filler if it was in a compact state or if the particles were fully dispersed. In case of clusters (agglomerates), the effective ϕ_2 is larger due to the presence of cavities even if the polymer does not wet the particles and get entrapped in these cavities. Care was taken to coat the filler particles with a chemically bound monolayer of stearic acid, avoiding the presence of excess surfactant (over-coating), which influences the mechanical properties of the composite [48]. The materials used and the sample preparation as well as the scanning electron microscopy (SEM) have been previously described [1]. The rheological properties were measured using a stress- and strain-controlled rheometer (MCR 300—Physica, Stuttgart, Germany) equipped with an electrically heated thermostating unit (TEK 350-CF). The experiments were carried out with a cone/plate geometry ($d=50$ mm, angle $=4°$, truncated 50 μm) at 170 °C under nitrogen. All samples ($d=20$ mm) were dried at 70 °C under reduced pressure over night. They were allowed to fully relax after squeezing in the rheometer (monitored by measuring the normal force) before starting the measurement. The strain-controlled experiments included dynamic strain (γ) sweep (logarithmically increasing from 0.04 to 100%) at a fixed angular frequency $\omega=1$ rad s^{-1} and small amplitude ($\gamma=0.052\%$) oscillatory shear measurements, in which ω was logarithmically increased from 0.02 to 600 rad s^{-1}. Both frequency and amplitude sweeps were carried out starting from the smallest values. Each sample underwent the following tests in sequence and in this order: Frequency

sweep (FS), amplitude sweep (AS) followed by a relaxation period of 0.5–1 h (depending on the filler concentration), frequency sweep and an amplitude sweep. The sample relaxation was monitored by observing the decrease in shear rate by time. For the frequency sweeps, a low amplitude ($\gamma = 0.052\%$) was chosen to ensure that the dynamic moduli are measured in the linear viscoelastic regime with the same amplitude for all filler concentrations. The average of three measurements for each sample is reported.

3. Results and discussion

In this part of the investigation, the results of rheological oscillatory shear experiments are presented and interpreted in terms of particle–particle and particle–matrix interactions. The parameters studied are filler loading, kneading intensity, preshear and surface treatment (stearic acid) of the filler. The effects of interparticle and particle–matrix interactions on polymer reinforcement as well as the mechanism of reinforcement are discussed in light of the obtained results.

Repetitive dynamic strain amplitude sweeps, in which the specimen was allowed to relax after each run, were carried out at a fixed ω of 1 rad s^{-1} for samples with filler loading ranging from 0 to 30 vol% (below the percolation limit of hard spheres). The complex viscosity $|\eta^*|$ measured in two consecutive runs is plotted as a function of the strain amplitude γ in Fig. 1 (for clarity only the high concentrations are shown). Since the shear stress develops almost linearly with the strain amplitude in the AS experiments, the $|\eta^*|$-stress plots look quite similar to those given in Fig. 1. For the 30 vol% untreated filler composite, a massive decrease of the zero shear viscosity $|\eta_0^*|$ was observed in the second run, whereas there is practically no difference in $|\eta^*|$ between the two runs at $\gamma = 90\%$. Measuring $|\eta^*|(\gamma)$ for the third time revealed no difference between the last two measurements, indicating that an irreversible (within 1 h) change in the microstructure occurred during the first AS and that additional shearing does not lead to a further change. The difference in the relative zero complex viscosity between the first and second run decreased with declining ϕ_2 (Fig. 2), pointing out that the viscosity reduction is related to a change in filler structure that develops with increasing loading. The viscosity reduction with shearing increased non-linearly but continuously with rising filler concentration and no threshold value was observed. Note that the filler volume fraction at 170 °C is smaller than at RT because of the decrease in polymer density across the melting point [1]. The viscoelastic linear regime was also smaller in the first run than in the second, especially at high ϕ_2 (Fig. 1). That is, the strain amplitude, corresponding to the onset of the non-linear viscoelasticity increased as a result of shearing in the first AS. This behavior implies breaking of certain linkages, strained beyond their elastic limits and correlate well with

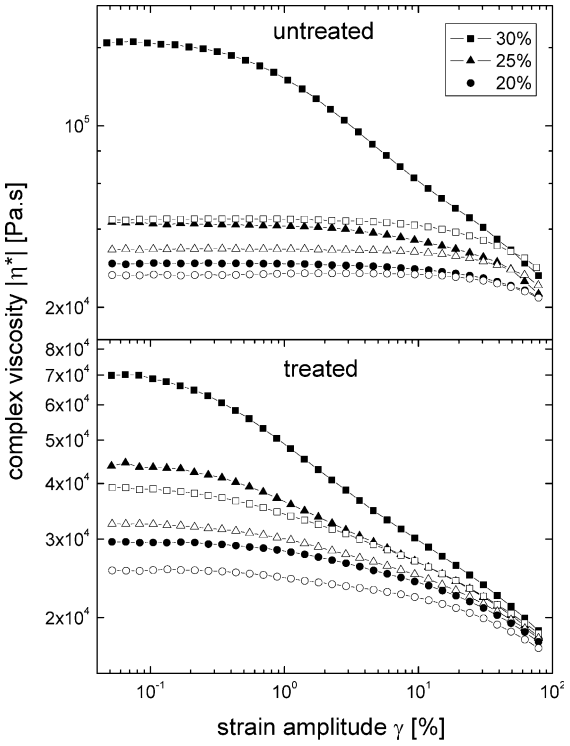

Fig. 1. Complex viscosity of calcite–HDPE composites (20–30 vol% treated and untreated filler) as a function of strain amplitude at 170 °C and $\omega = 1$ rad s^{-1}. Full symbols represent the first measurement, while open symbols stand for the 2nd run after relaxation.

the steady shear results obtained in the first part of this investigation that indicated the presence of filler agglomerates (clusters) with a size distribution (Fig. 3), whose number and size increase with increasing ϕ_2 [1]. These clusters disintegrate to smaller clusters or primary particles on shearing, leading to lower viscosity. Depending on the size and number of the clusters as well as on the attraction forces between the primary particles, corresponding shear stresses are needed to take them apart. The onset amplitude

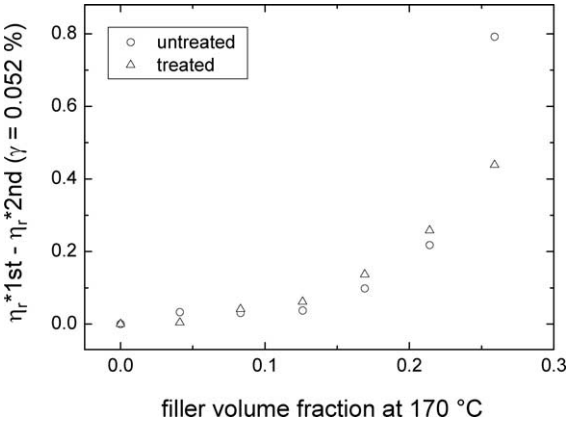

Fig. 2. Difference between the relative shear complex viscosities ($\gamma = 0.052\%$) of treated and untreated calcite–HDPE composites measured in the 1st and 2nd amplitude sweeps as a function of filler volume fraction at 170 °C.

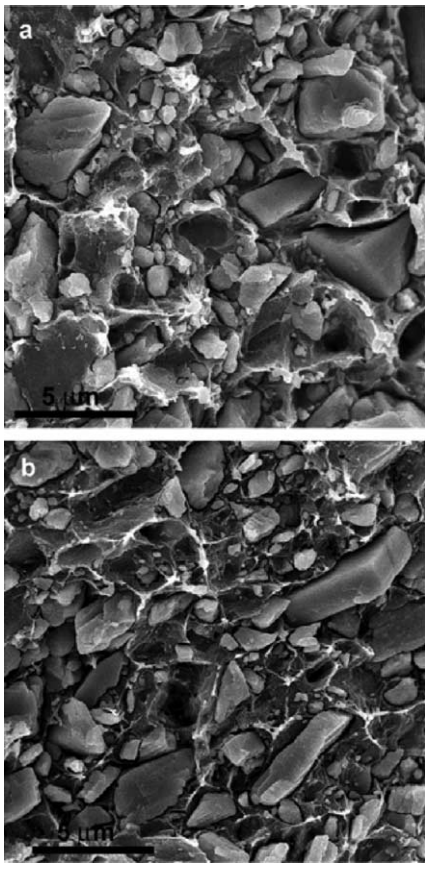

Fig. 3. SEM micrographs of cryo-fractured samples of 30 vol%, (a) untreated, (b) surface treated, $CaCO_3$–HDPE composites.

of the non-linear viscoelasticity is reduced by the presence of filler clusters due to their disintegration at low γ. In other words, the presence of filler clusters increases the viscosity and enhances the viscoelastic non-linearity. The high $|\eta_0^*|$ of the 30 vol% untreated filler composite and the large difference between the first and second run correspond to the divergent shear viscosity and the so called 'apparent yield' that was observed in the steady shear measurements [1]. The shear thinning that occurred with increasing strain amplitude was also enhanced at high ϕ_2 as observed in steady shear measurements. The composites of the surface treated filler showed slightly lower $|\eta_0^*|$ than that of the untreated calcite composites (except for the 30% composite that showed a remarkable difference) and the decrease in viscosity due to preshearing was less dramatic (Fig. 1, note the different scales). It is reasonable to assume that the number of clusters in the treated filler composites is smaller than in those of the untreated filler. That is, the surface treatment reduces the agglomeration to a large extent but does not hinder it completely and shearing destroys the residual clusters. Agglomerates of treated particles are expected to be weaker and need less shear forces to be disintegrated than those of the untreated filler because the dipole–dipole interactions that exist between the untreated particles are stronger than the dispersion forces between the stearyl chains and PE. The difference between $|\eta_0^*|$ of the 30 vol% treated and untreated filler composites in the 2nd run (after preshear) is small, confirming that the effect of surface treatment on the viscosity can be mainly ascribed to the reduction of agglomeration. Comparing the 2nd run curves of the untreated calcite composites with those of the treated filler shows that strong shear thinning occurs in the latter although no particle disintegration takes place. This can be attributed to interfacial slippage that occurs due to the decreased particle–matrix interactions [1,45]. The viscoelastic linear regime in the treated filler composites was also generally smaller than in those of the untreated filler and was not broadened by the shear in the first AS, supporting the notion that interfacial slippage occurs in the treated filler composites.

To confirm the effect of agglomerates, 20 and 30 vol% untreated calcite compounds, in which the last kneading step at 60 rpm was skipped, i.e. less sheared during compounding, were prepared and in the following denoted 'agg' [1]. Fig. 4 compares the viscoelastic behavior of these composites with those of the composites prepared by the standard method (less agglomerated). The 'agg' compounds showed higher $|\eta_0^*|$ than the standard ones and the difference gradually diminished with increasing strain amplitude to reach the same viscosity at the highest amplitude. These results confirm the presence of agglomerates (clusters), with consequences for the viscosity, and that they are disintegrated during the AS. The increased viscosity in both 'agg' samples (20 and 30 vol%) compared to the corresponding standard ones as well as the gradual increase of this effect with augmenting ϕ_2 confirms the presence of clusters (local structure) and disapproves the perception of space-filling filler network at these concentrations. It can also be seen in Fig. 4 that increased agglomeration reduces the linear viscoelastic range, confirming the contribution of clusters to the viscoelastic non-linearity. In Fig. 5, rheological response of the 25 vol% composite measured in the first and second AS is compared to that of samples that were steady

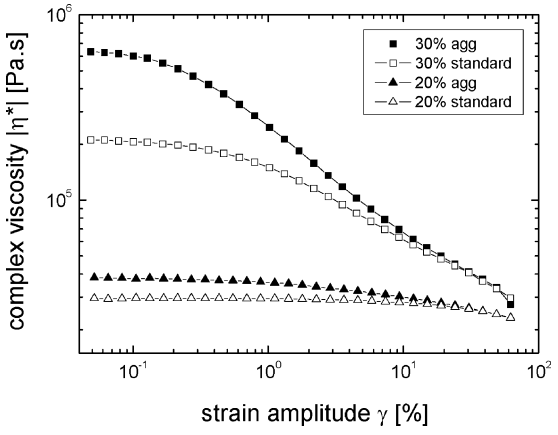

Fig. 4. Comparison of the complex viscosity of agglomerated and standard 20 and 30 vol% calcite–HDPE composites as a function of strain amplitude at 170 °C and $\omega = 1$ rad s^{-1}.

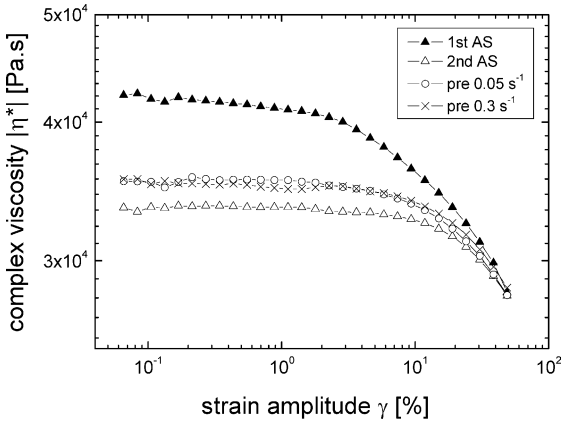

Fig. 5. Comparison of the viscoelasticity (AS) of 25 vol% composites with and without steady preshear ($\dot{\gamma} = 0.05$ or 0.3 s^{-1}) at 170 °C.

presheared at shear rates $\dot{\gamma} = 0.052$ or 0.3 s^{-1} for 5 min, then left quiescent for 30 min prior to the measurement. As can be seen, the steady preshear disintegrated the clusters to a great extent, leading to lower viscosity but the sinusoidal stress that ranged from 10 to 21,000 Pa, corresponding to $\dot{\gamma} = 0.0002 - 1.07$ s^{-1}, over a period of 13 min (duration of the AS) was more effective in destroying the clusters. It has been shown by SEM that the number of clusters in the standard compounds is limited and that they are destroyed to a great extent by the steady preshear [1]. The shear forces of the first AS reduced the viscosity further, so that it can be assumed that the few clusters present were completely disintegrated by the oscillatory shear. The fact that the decrease in $|\eta_0^*|$ of the untreated $CaCO_3$ is the same as that of the weakly agglomerated treated filler up to 15 vol% (Fig. 2) also supports this assumption.

In the oscillatory measurements, the storage (G') and loss (G'') moduli of the composites were functions of the strain amplitude (γ) and showed a linear region followed by a non-linear one, in which they decreased with increasing strain amplitude similar to the viscosity. The slope of the non-linear part increased and the linear range decreased with increasing filler volume fraction. Both moduli increased with rising ϕ_2 but the G'-dependency was larger than that of G''. To visualize this effect, the reduced moduli (composite/HDPE) G_r' and G_r'' at $\gamma = 0.052$ and 49% are plotted as functions of ϕ_2 in Figs. 6 and 7 (note the different Y-scales). At the high strain amplitude, i.e. after cluster disintegration, G_r' of the untreated filler composites is the same in both runs and the filler surface treatment reduces it (Fig. 6). At the low strain amplitude, G_r' of the untreated filler composites increases exponentially with rising ϕ_2 in the first run, showing the effect of clusters on the polymer stiffness. The reduction of this contribution after filler surface treatment confirms the effect of clusters. In the 2nd run, i.e. in absence of clusters, the $G_r' - \phi_2$ dependency is also much smaller. G_r'' shows a similar behavior to that of G_r' (Fig. 7), however G_r' increases faster with increasing ϕ_2. At $\gamma = 0.052\%$ G_r' is twice as high as G_r'' in the 1st run, indicating that the

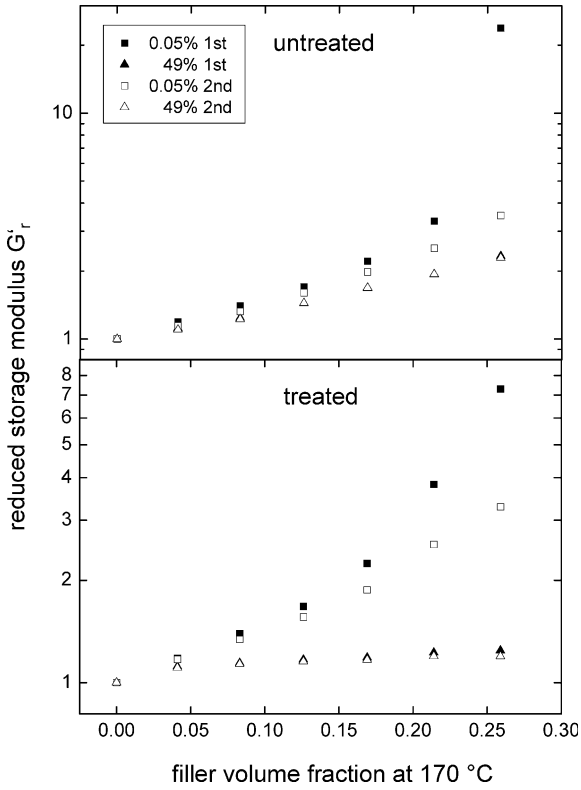

Fig. 6. Reduced storage modulus of treated and untreated calcite–HDPE composites at $\gamma = 0.052$ and 49% ($\omega = 1$ rad s^{-1}) as a function of filler volume fraction at 170 °C, 1st stands for the first AS and 2nd for the second run after a relaxation period.

agglomerates also have stronger influence on the storage modulus. The loss tangent $\tan\delta$ (G''/G') is plotted in Fig. 8 as a function of γ for the untreated and treated filler composites with (2nd run) and without (1st run) preshearing summing up the effect of the inclusions on the composite moduli. At low amplitudes, $\tan\delta$ decreases with increasing ϕ_2 and that of the 30% composite is smaller in the 1st run than in the 2nd, showing the influence of primary particles and clusters on the moduli. Surface treatment of the filler reduces the linear region and increases $\tan\delta$ of the composites at high strain amplitudes above that of the polymer, pointing out that interfacial slippage takes place. The difference between the two runs in the treated calcite composites indicates that some clusters were present at large ϕ_2 and were disintegrated during the first AS.

It is well recognized that small-amplitude oscillatory shear does not significantly deform the microstructure of a complex fluid, hence allows exploring the effect of the fluid structure on the viscosity and moduli [49]. The $|\eta^*|(\omega)$ at $\gamma = 0.052\%$ of treated and untreated calcite–HDPE composites with different filler loading, before and after an AS (preshear) followed by a relaxation period, is plotted in Fig. 9. At high filler loading, a distinct reduction in $|\eta_0^*|$ over the whole frequency range, although more pronounced at low frequencies, can be observed as a result of preshearing (disintegration of the clusters). However, this effect

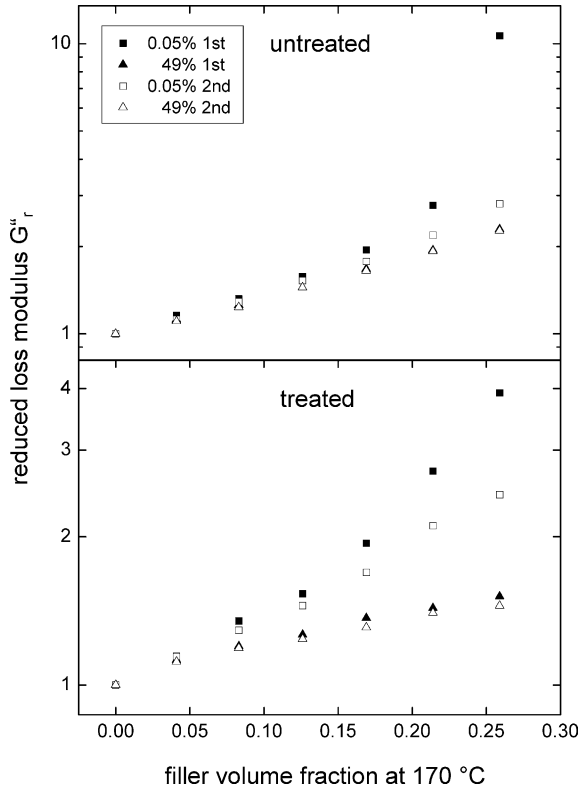

Fig. 7. Reduced loss modulus of treated and untreated calcite–HDPE composites at $\gamma = 0.052$ and 49% ($\omega = 1$ rad s^{-1}) as a function of filler volume fraction at 170 °C, 1st stands for the first AS and 2nd for the second run after a relaxation period.

diminishes with decreasing filler volume fraction in accordance with the expectation of fewer agglomerates at low loading. The frequency dependence before preshearing was reproducible (back and forth) and that after the AS as well, confirming that the small-amplitude oscillation does not deform the microstructure and that the deformation induced by the AS is irreversible (within 1 h). In the low frequency range, the slope of the curves changes as a result of preshearing, leading to a splay between the two curves (1st and 2nd run). These observations are valid for both treated and untreated filler composites but to different extents and underline the influence of agglomerates on the viscoelasticity of the complex fluid. Since the degree of agglomeration depends on many factors including the processing conditions, the reinforcing effect of primary particles should be considered decoupled from that of the clusters.

To study the filler reinforcing effect, the linear storage and loss moduli of the composites were measured with and without preshearing. As an example $G'(\omega)$ and $G''(\omega)$ of the 25 and 30 vol% composites are plotted in Fig. 10. At low frequencies, the moduli increase and the slopes of the curves gradually decrease with increasing ϕ_2, tending towards a solid-like behavior at high filler loading. The slopes of the $G'(\omega)$ and $G''(\omega)$ log-plots are similar in the terminal zone, however with increasing frequency G' increases faster than

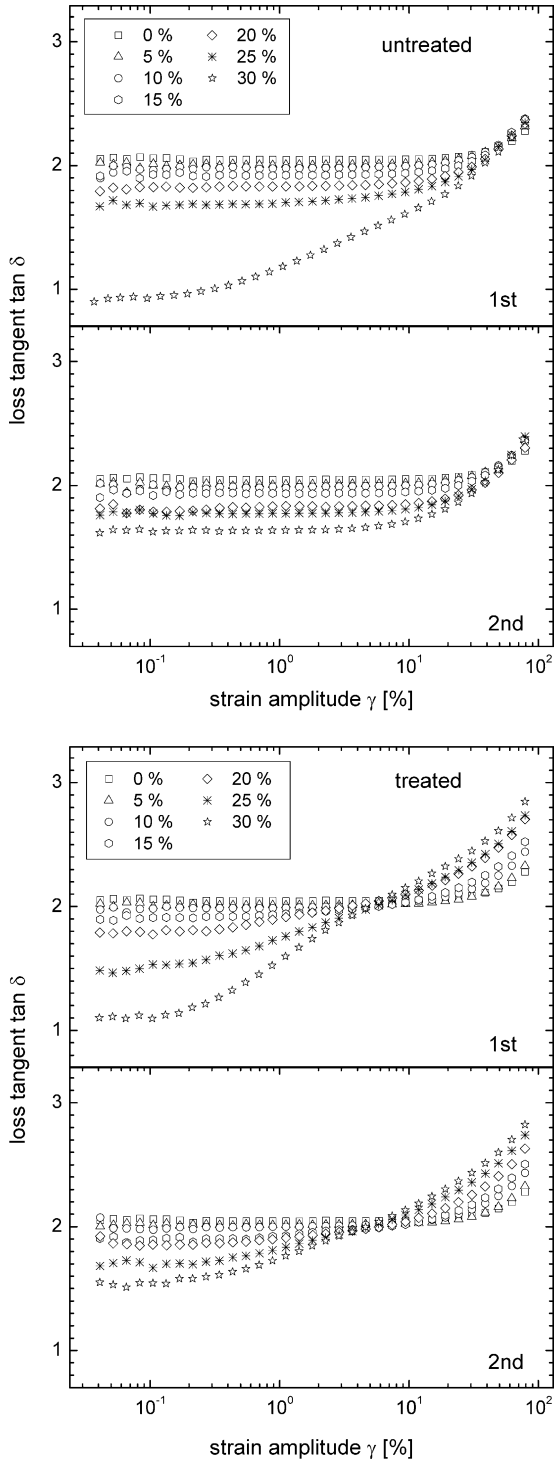

Fig. 8. Loss tangent $\tan\delta$ of treated and untreated calcite–HDPE composites plotted as a function of the strain amplitude ($\omega = 1$ rad s^{-1}), 1st stands for the first AS and 2nd for the second run after a relaxation period.

G'' and the slope of $G''(\omega)$ decreases, so that the two curves cross each other at a certain frequency ω_c, marking a transition from liquid-like to solid-like response and G' becomes larger than G''. The same trend was observed in composites with different loading but the curves shifted

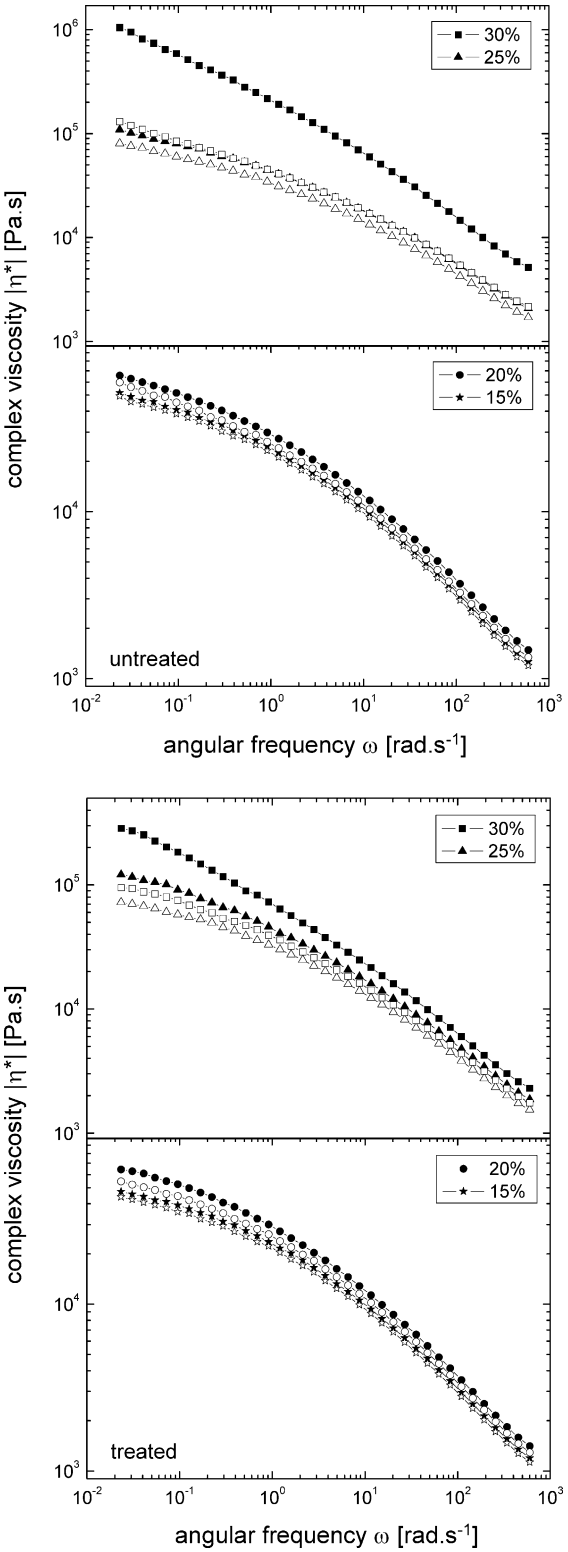

Fig. 9. Complex viscosity of calcite–HDPE composites (15–30 vol% treated and untreated filler) as a function of the angular frequency at 170 °C ($\gamma = 0.052\%$). Full symbols represent the first run on a virgin sample, while open symbols stand for the second measurement after an amplitude sweep followed by a relaxation period.

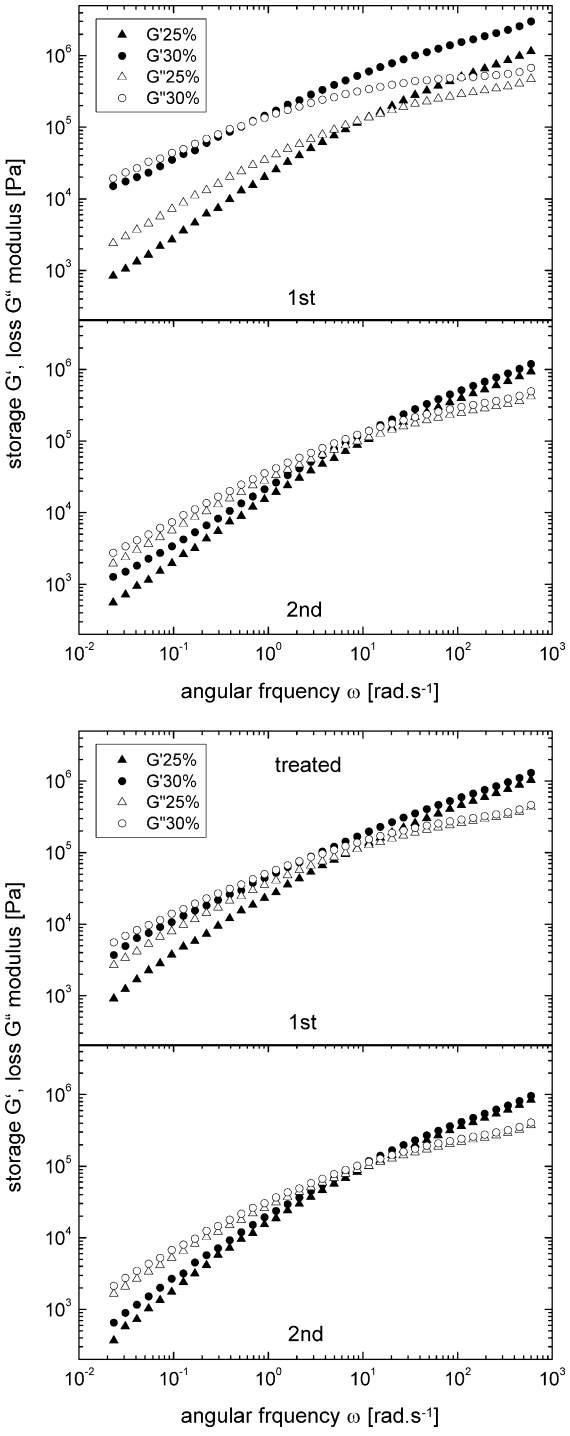

Fig. 10. Storage and loss moduli of treated and untreated calcite–HDPE composites (25 and 30 vol%) plotted as a function of the angular frequency at 170 °C ($\gamma = 0.052\%$). 1st stands for the first FS and 2nd for the second run after an AS and a relaxation period.

toward lower frequencies and higher moduli with increasing ϕ_2 as a result of the increase in relaxation time (ω_c is approximately equal to the inverse of the fluid's characteristic relaxation time λ_c, roughly the longest time required for the elastic structures in the fluid to relax). This led to a shift of ω_c, where $G' = G''$, to lower values with increasing ϕ_2

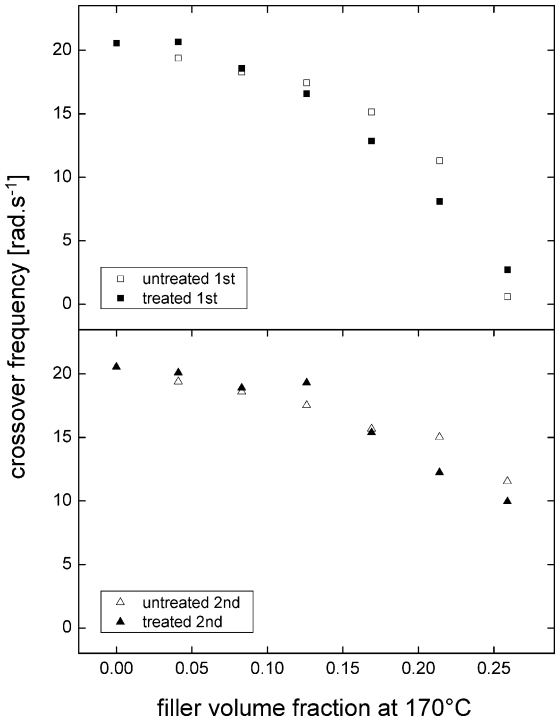

Fig. 11. Dependence of the crossover frequency ω_c of treated and untreated calcite–HDPE composites ($\gamma = 0.052\%$), 1st stands for the first FS and 2nd for the second run after an AS and a relaxation period.

similar to that observed in elastomers with increasing cross-linking, which converts their response from that of a viscoelastic liquid to that of a viscoelastic solid. The shift in crossover frequency toward lower values with increasing ϕ_2 was also observed in the 2nd run measurements (primary particles) but on a smaller scale. To visualize this effect, ω_c is plotted as a function of ϕ_2 in Fig. 11. It can be seen that increasing the volume fraction of primary particles (2nd run) leads to a gradual non-linear decrease of ω_c that corresponds to increasing relaxation times, indicating less flexibility of the polymer chains. An additional contribution results from the presence of clusters (1st run) and the ω_c decay is accelerated, hence reaching very small values. The decay is exponential and no threshold value is observed. Below 20 vol% filler loading, the surface treatment seems to have little or no influence on this slow relaxation process, suggesting a topological origin of the long relaxation time. It is to be noted that above ω_c, the $G'' - \omega$ dependency is small (Fig. 10) and becomes marginal at high concentrations of the untreated filler, i.e. in presence of clusters. It seems that the inclusions introduce topological restraints to the reptation of the polymer chains (responsible for long relaxation times) and the clusters represent larger obstacles than the primary particles, which is reflected in energy dissipation.

In Fig. 12, the loss tangent tan δ is plotted as a function of ω for the untreated and treated filler composites with and without preshearing. Similar tan $\delta - \omega$ correlations can be

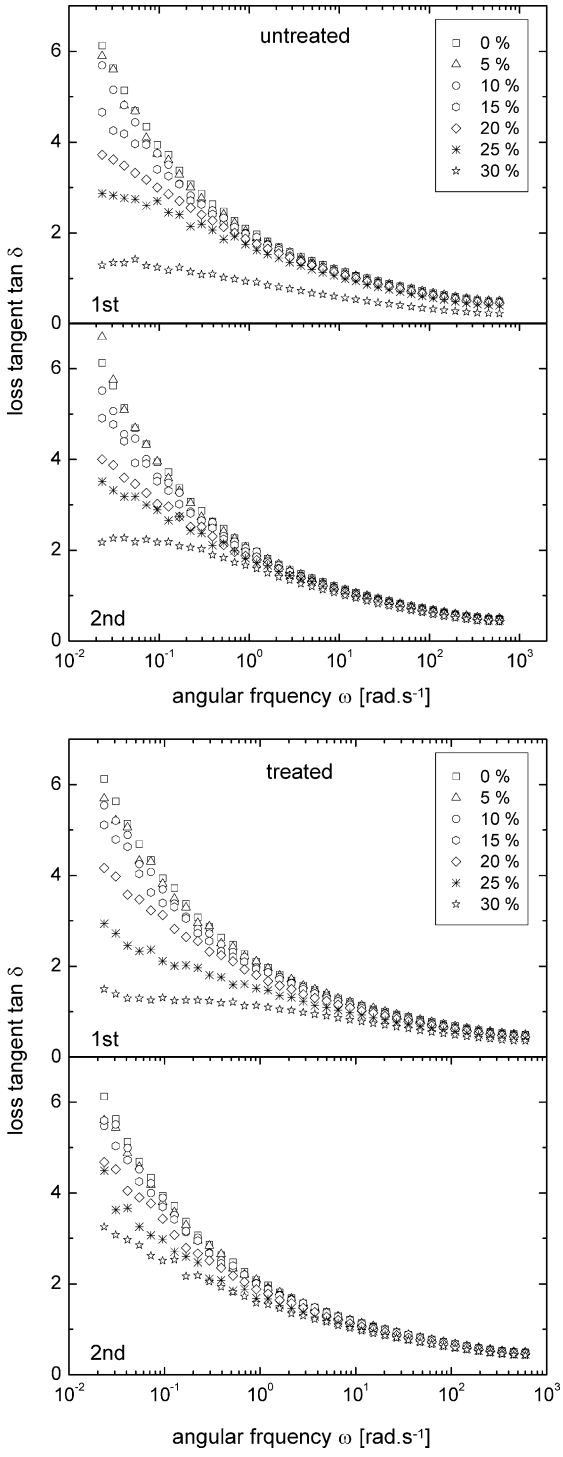

Fig. 12. Loss tangent tan δ plotted as a function of the angular frequency for treated and untreated calcite–HDPE composites ($\gamma = 0.052\%$), 1st stands for the first FS and 2nd for the second run after an AS and a relaxation period.

seen at low filler loading and a fast decay in tan δ (G''/G') is observed due to the fact that G' increases faster than G'' with increasing frequency (Fig. 10). However, a divergence in magnitude and ω-dependency can be observed in the terminal region with increasing filler loading. This is due

to the facts that G' increases faster than G'' and the $G'-\omega$ dependency becomes larger than that of G'' with increasing ϕ_2 (Fig. 10). The magnitude of tan δ is also lower in the 1st run than in the 2nd and in the untreated filler composites than in those of the treated one due to the presence of clusters, indicating that clusters increase G' more than G'' (Fig. 10). This leads to low tan δ values and a decrease in the ω-dependency. For these reasons, tan δ of the 30% composite is practically frequency independent in all cases below $\omega \approx 0.2$ rad s^{-1} except for the 2nd run of the treated filler composite. The slope of the tan $\delta-\omega$ dependency as well as the tan δ values also increased with surface treatment of the filler similar to what was observed with increasing strain amplitude (Fig. 8).

The reduced linear storage modulus G'_r (composite/matrix) measured by small-amplitude oscillatory shear (FS) with (2nd run) and without (1st) sinusoidal preshear is plotted in Fig. 13 as a function of ω. The exponential increase of G'_r with decreasing ω as well as with increasing ϕ_2 reflects the tendency towards a solid-like behavior at low frequency with increasing filler loading that was observed in Fig. 10. Within the same run, G'_r is a function of ω at low frequencies but the dependence decreases with increasing ω. The $G'_r-\omega$ dependency also diminishes with decreasing filler loading, so that the reduced shear modulus becomes frequency independent in the high frequency region at

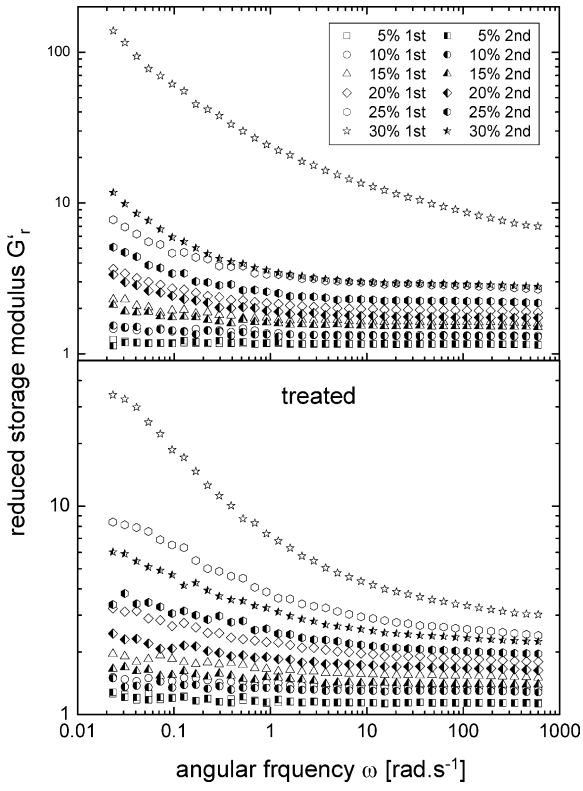

Fig. 13. Reduced storage modulus of 5–30 vol% treated and untreated calcite–HDPE composites plotted as a function of the angular frequency ($\gamma=0.052\%$) at 170 °C. 1st stands for the first FS and 2nd for the second run after an AS and a relaxation period.

$\phi_2 \lesssim 20\%$ and over the whole frequency range at $\phi_2 \lesssim 5\%$. Since the hydrodynamic contribution is an instantaneous stress that should be the same at any frequency, these results indicate that at high frequencies the hydrodynamic reinforcement is dominant [50,51]. The fact that G'_r is generally larger in the low frequency region than at high ω indicates that other forces offer an additional contribution to the modulus. Since small-amplitude oscillatory shear does not significantly deform the microstructure and the additional reinforcement is observed in both runs, this frequency sensitive contribution cannot be related to a change in filler structure. The contribution also decreases with filler surface treatment in the 2nd run (compare 2nd run treated and untreated), which suggests that it can be attributed to particle–matrix interactions, i.e. polymer adsorption on the filler surface (transient filler–polymer network controlled by association and dissociation of reversible linkages). At equilibrium (frequency dependant), the strands of the transient network support the stress and store elastic energy as in a permanently cross-linked network. The dynamics of the adsorbed polymer chains are also different from that of the bulk-polymer [32,52]. Polymer adsorption is expected to increase the effective ϕ_2 and to be stronger in untreated calcite composites than in those of the treated filler. The dipole-induced dipole attraction forces between the calcite particles and the polymer chains are reduced by the surface treatment because the coating layer keeps the polymer at a distance r from the calcite surface and the attraction force is inversely proportional to r^6. The attractive dispersion forces between the alkyl chains of the coating layer and PE are weak and the short (C_{18}) alkyl chains cannot entangle with the polymer chains. That is, the interfacial adhesion between the treated filler particles and the polymer is weak; hence the organic coating reduces the polymer adsorption and lubricates the flow of the polymer melt, decreasing the filler contribution to G'_r. The difference between the curves of the 1st and 2nd runs, which becomes obvious at $\phi_2 \gtrsim 15\%$, is probably due to the slow relaxation processes observed in Figs. 10 and 11. This difference decreases as a result of filler surface treatment because the viscoelastic properties in the terminal zone are dominated by the longest relaxation times that are determined by long-range motions. That is, the additional reinforcing contribution at low frequencies stems from the polymer adsorption to the filler surface and from the topological restraints introduced by the primary particles and the clusters, leading to slow relaxation of the polymer chains and more energy storage than dissipation.

To better visualize the development of G'_r with increasing ϕ_2, G'_r at $\omega=0.031$ and 453 rad s^{-1} is plotted as a function of ϕ_2 for virgin (1st) and presheared (2nd) specimens of treated and untreated calcite–HDPE composites in Fig. 14. In all cases, G'_r is a non-linear function of the filler volume fraction. The curve 453 2nd represents the hydrodynamic reinforcement by the primary particles. The

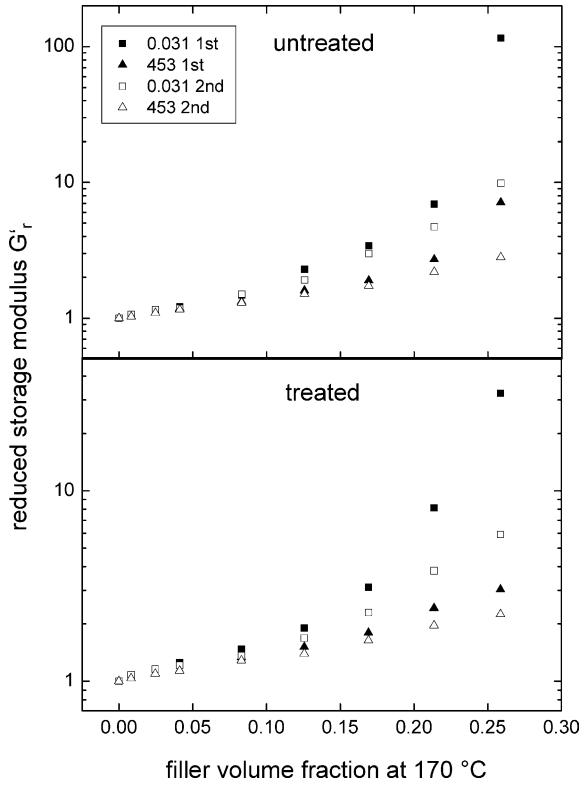

Fig. 14. Reduced storage modulus of treated and untreated calcite–HDPE composites at $\omega = 0.031$ and 453 ($\gamma = 0.052\%$) as a function of filler volume fraction at 170 °C. 1st stands for the first FS and 2nd for the second run after an AS and a relaxation period.

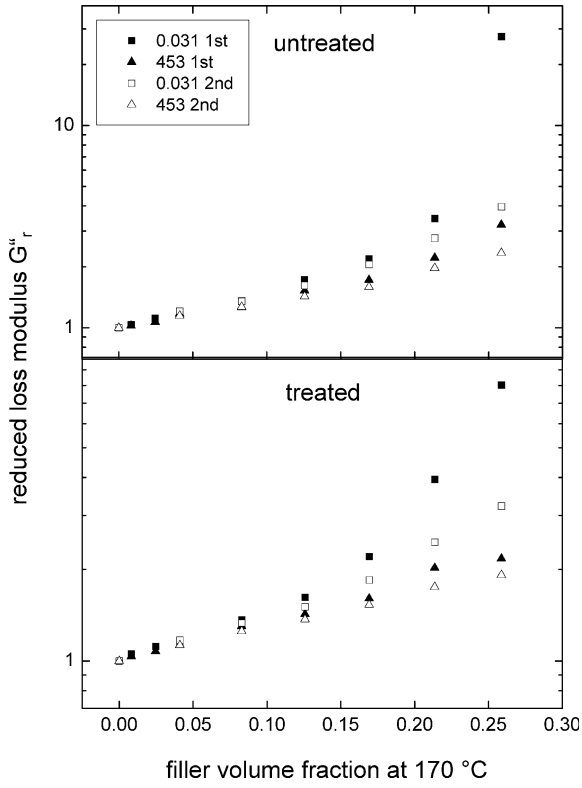

Fig. 15. Reduced loss modulus of treated and untreated calcite–HDPE composites at $\omega = 0.031$ and 453 ($\gamma = 0.052\%$) as a function of filler volume fraction at 170 °C. 1st stands for the first FS and 2nd for the second run after an AS and a relaxation period.

stearic acid coating of the particles reduces this contribution. The curve 453 1st shows the hydrodynamic contribution of the filler before shearing (primary particles and clusters) to G'_r. At $\phi_2 \lesssim 10\%$, there is little or practically no difference in G'_r between the first and second run, indicating the absence (or presence of very few) clusters. Above this concentration, the hydrodynamic contribution of the clusters to the stiffness is noticeable. This effect is smaller in the surface treated filler composites, confirming that the surface treatment reduces the tendency to agglomeration. Note that clusters beside increasing the effective ϕ_2 have different shapes and packing than the primary particles, leading to larger $[G]$ and smaller ϕ_{max} [9,53,54]. The reinforcing effect of the primary particles (0.031 2nd) is larger at low frequency than at high ω (453 2nd), showing the contribution of polymer adsorption to the linear shear modulus and of the restraints exerted on the polymer relaxation by the presence of inclusions. A marked increase in modulus can be seen in the first run at $\omega = 0.031$, especially at high filler loading due to the presence of clusters. This reinforcement decreases with diminishing agglomeration in the surface treated filler composites. The sum of these effects leads to the observed tendency towards a solid-like response at high ϕ_2 and small ω. The reduced loss modulus G''_r showed the same behavior as G'_r but on a smaller scale because of the weaker influence of the filler on G''_r (Fig. 15). This led to higher G'_r than G''_r at filler volume fractions above 15%. It is noteworthy that the stronger filler influence on G'_r is more pronounced in the FS measurements than in the AS. In presence of inclusions, energy is more stored than dissipated, however, in the AS a part of the energy is consumed in cluster disintegration.

Fitting the $G'_r(\phi_2)$ and $G''_r(\phi_2)$ data obtained from the small amplitude oscillatory shear measurements in the second run (presheared) to Eq. (2) (hydrodynamic model) and Eq. (4) (micromechanical model), gave values for $[G]$, ϕ_{max}, A and ψ, which are listed in Tables 1 and 2. In the 2nd run (Table 1), the clusters are already disintegrated and the primary particles are nearly spherical. For the untreated filler composites, where the adhesion between the polymer and the particles is strong, the assumptions underlying the models are fulfilled. At high frequency ($\omega = 453$ rad s^{-1}), the hydrodynamic reinforcement is dominant and the expected values for hard spheres are obtained [9,53–55]. At low-frequency ($\omega = 0.031$ rad s^{-1}), where the slow relaxation processes contribute to the polymer stiffness, high values for $[G]$ and A as well as low values for ϕ_{max} and ψ were calculated. The filler surface treatment did not have a strong influence on the fit parameters at low-frequency but led to irrational values of ϕ_{max} and ψ at $\omega = 453$ rad s^{-1}, probably due to the interfacial slippage at high frequency. Fitting the $G'_r(\phi_2)$ and $G''_r(\phi_2)$ data obtained from the first run (primary particles and clusters) to Eqs. (2) and (4), gave

Table 1
Parameters obtained by fitting the reduced storage and loss moduli of presheared specimens (2nd run) of treated and untreated calcite–HDPE composites, measured by small-amplitude oscillatory shear, to Eqs. (2) and (4)

Frequency (rad s^{-1})	Module	Untreated				Treated			
		$[G]$	A	ϕ_{max}	ψ	$[G]$	A	ϕ_{max}	ψ
453	G_r'	2.71	1.82	0.46	0.42	2.72	1.85	1.01	0.57
	G_r''	2.47	1.56	0.57	0.49	2.54	1.70	$\gg 1$	1.16
0.031	G_r'	4.48	4.67	0.33	0.31	3.99	3.56	0.37	0.33
	G_r''	3.31	2.56	0.40	0.36	2.95	2.08	0.43	0.39

$[G]$, intrinsic modulus; ϕ_{max}, maximum packing fraction; A, fit parameter that takes the geometry of the particles and Poisson's ratio of the matrix into account; ψ, fit parameter that depends on ϕ_{max}.

small values for ϕ_{max} and ψ as expected for clusters of different shape and packing (Table 2). However, some of the calculated parameters cannot be rationalized, indicating that the presence of clusters is not foreseen in these models. That is, both models are well suited to predict the hydrodynamic reinforcing effect of primary spherical particles, to which polymers stick but are unable to forecast the influence of the slow relaxation processes present in polymer composites. If the interfacial adhesion forces between the polymer and the inclusions are weak, these models lead to irrational results.

4. Conclusions

Above a certain volume fraction (in this case 10 vol%), calcite particles tend to agglomerate in HDPE giving clusters, which disintegrate on shearing during amplitude sweep experiments. The presence of clusters increases the viscosity and moduli of the composites beyond the expected reinforcement by primary particles. Clusters also reduce the onset amplitude of the non-linear viscoelasticity due to their disintegration at low strain amplitudes. Coating the calcite particles by a stearic acid monolayer reduces their tendency to agglomerate as well as the interfacial adhesion forces between the particles and the polymer. The latter leads to interfacial slippage with increasing strain amplitude and enhances the viscoelastic non-linearity. The hydrodynamic contribution to the polymer reinforcement is frequency independent and dominates at high frequency. The polymer adsorption on the filler surface (transient network, polymer immobilization and higher effective ϕ_2) as well as the topological restraints exerted by the inclusions on the polymer chain reptation lead to slow relaxation, hence contributes to the moduli of the composites. These slow relaxation processes are sensitive to the oscillation frequency and contribute to the polymer reinforcement in the terminal region. They also lead to a shift of the crossover (liquid-like to solid-like) frequency to lower values with increasing filler volume fraction. Agglomerates differ in shape and packing from the nearly spherical primary particles, and exert large restraints on the polymer chain relaxation, thus contribute to the composites' moduli. The sum of these factors leads to the observed tendency towards a solid-like response in the terminal zone. Primary particles, and clusters even more, have stronger influence on G' than on G'', hence lead to lower tan δ. The hydrodynamic and micromechanical models can only predict the hydrodynamic reinforcement in untreated filler composites, where the polymer strongly adheres to the particles surface.

Acknowledgements

We gratefully acknowledge financial support from the Swiss National Science Foundation (SNF).

Table 2
Parameters obtained by fitting the reduced storage and loss moduli of treated and untreated calcite–HDPE composites (1st run), measured by small-amplitude oscillatory shear, to Eqs. (2) and (4)

Angular frequency (rad s^{-1})	Reduced module	Untreated				Treated			
		$[G]$	A	ϕ_{max}	ψ	$[G]$	A	ϕ_{max}	ψ
453	G_r'	2.42	0.49	0.27	0.29	2.99	2.16	0.48	0.41
	G_r''	2.39	1.26	0.34	0.36	2.95	2.08	3.82	0.69
0.031	G_r'	4.42	4.80	0.26	0.26	5.23	7.02	0.29	0.27
	G_r''	2.83	0.58	0.26	0.27	3.57	2.67	0.30	0.30

Symbols as Table 1.

References

[1] Osman MA, Atallah A, Schweizer T, Öttinger HC. J Rheol 2004;48: 1167.
[2] Hill R, Power G. QJ Mech Appl Math 1956;9:313.
[3] Smallwood HM. J Appl Phys 1944;15:758.
[4] Guth E. J Appl Phys 1945;16:20.
[5] Hashin Z. Proceedings of the 4th international congress on rheology. New York: Interscience; 1965. p. 30 [Part 3].
[6] Krieger IM, Dougherty TJ. Trans Soc Rheol 1959;3:137.
[7] Krieger IM. Adv Colloid Interface Sci 1972;3:111.
[8] Choi GN, Krieger IM. J Colloid Interface Sci 1986;113:101.
[9] Douglas JF, Garboczi EJ. Adv Chem Phys 1995;41:85.
[10] Sudduth RD. Mater Sci Technol 2003;19:1181.
[11] Kerner EH. Proc Phys Soc 1956;B69:808.
[12] Hashin Z, Shtrikman S. J Mech Phys Solids 1963;11:127.
[13] Halpin JC. J Compos Mater 1969;3:732.
[14] Nielsen LE. J Compos Mater 1967;1:100.
[15] Lewis TB, Nielsen LE. J Appl Polym Sci 1970;14:1449.
[16] Nielsen LE. J Appl Phys 1970;41:4626.
[17] Pukánszky B. Polypropylene structure, blends and composites. vol. 3. London: Chapman & Hall; 1995.
[18] Vollenberg PHT, Heikens D. Polymer 1989;30:1656.
[19] Fu Q, Wang G, Liu C. Polymer 1995;36(12):2397.
[20] Payne AR, Whittaker RE. Rubber Chem Technol 1971;44:440.
[21] Leonov AI. J Rheol 1990;24:1039.
[22] Coussot P, Leonov AI, Piau JM. J Non-Newt Fluid Mech 1993;46: 179.
[23] Eggers H, Schümmer P. Rubber Chem Technol 1996;69:253.
[24] Donnet JB. Rubber Chem Technol 1998;71:323.
[25] Sternstein SS, Zhu AJ. Macromolecules 2002;35:7262.
[26] Heinrich G, Kluppel M. Adv Polym Sci 2002;160:1.
[27] Le Meins JF, Moldenaers P, Mewis J. Ind Eng Chem Res 2002;41: 6297.
[28] Havet G, Isayev AI. Rheol Acta 2003;42:47.
[29] Sarvestani AS, Picu CR. Polymer 2004;45:7779.
[30] Aral BK, Kalyon DM. J Rheol 1997;41:599.
[31] Wolf S, Wang MJ. Rubber Chem Technol 1992;65:329.
[32] Picu RC, Ozmusul MS. J Chem Phys 2003;118:11239.
[33] Wang SQ, Inn YW. Rheol Acta 1993;32:581.
[34] Inn YW, Wang SQ. Phys Rev Lett 1996;76:467.
[35] Simhambhatla M, Leonov AI. Rheol Acta 1995;34:329.
[36] Aranguren MI, Mora E, DeGroot JV, Macosko CW. J Rheol 1992;36: 1165.
[37] Lobe VM, White JL. Polym Eng Sci 1979;19:617.
[38] Gandhi K, Salovey R. Polym Eng Sci 1988;28:877.
[39] Li L, Masuda T. Polym Eng Sci 1990;30:841.
[40] Wang Y, Wang JJ. Polym Eng Sci 1999;39:190.
[41] Wang Y, Yu MJ. Polym Compos 2000;21:1.
[42] Sun L, Park M, Salovey R, Aklonis JJ. Polym Eng Sci 1992;32:777.
[43] Suetsugu Y, White JL. J Appl Polym Sci 1983;28:1481.
[44] Malik TM, Carreau PJ, Germela M, Dufresne A. Polym Compos 1988;9:412.
[45] Inn YW, Wang SQ. Langmuir 1995;11:1589.
[46] Wang SQ, Inn YW. Polym Int 1995;37:153.
[47] Osman MA, Suter UW. Chem Mater 2002;14:4408.
[48] Osman MA, Atallah A, Suter UW. Polymer 2004;45:1177.
[49] Larson RG. The structure and rheology of complex fluids. New York: Oxford University Press; 1999.
[50] Brady JF. J Chem Phys 1993;99:567.
[51] Kuelpmann A, Osman MA, Kocher L, Suter UW. Polymer 2005;46: 523.
[52] Vilgis TA. Polymer 2005;46:4223.
[53] Jeffrey DJ, Acrivos A. AICHE J 1976;22:417.
[54] Bicerano J, Douglas JF, Brune DA. JMS-Rev Macromol Chem Phys 1999;C39(4):561.
[55] Christensen RM. Compos B 2004;35:475.